Mercury isotopes as tracers of ecology and metabolism in two sympatric shark species

Gaël Le Croizier, Anne Lorrain, Jeroen E. Sonke, Sébastien Jaquemet, Gauthier Schaal, Marina Renedo, Lucien Besnard, Yves Cherel, David Point

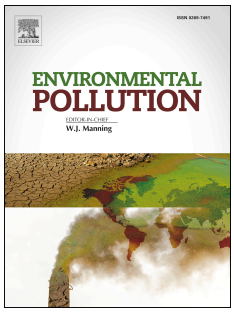

Mercury isotopes as tracers of ecology and metabolism in two sympatric shark species

Gaël Le Croizier, Anne Lorrain, Jeroen E. Sonke, Sébastien Jaquemet, Gauthier Schaal, Marina Renedo, Lucien Besnard, Yves Cherel, David Point

PII: S0269-7491(20)33198-5

DOI: https://doi.org/10.1016/j.envpol.2020.114931

Reference: ENPO 114931

To appear in: *Environmental Pollution*

Received Date: 27 April 2020

Revised Date: 27 May 2020

Accepted Date: 1 June 2020

Please cite this article as: Le Croizier, Gaë., Lorrain, A., Sonke, J.E., Jaquemet, Sé., Schaal, G., Renedo, M., Besnard, L., Cherel, Y., Point, D., Mercury isotopes as tracers of ecology and metabolism in two sympatric shark species, *Environmental Pollution* (2020), doi: https://doi.org/10.1016/j.envpol.2020.114931.

Gaël Le Croizier: Conceptualization, Methodology, Formal analysis, Writing - Original Draft, Writing - Review & Editing. **Anne Lorrain**: Resources, Writing - Review & Editing, Supervision, Funding acquisition. **Jeroen Sonke**: Formal analysis, Resources, Writing - Review & Editing, Supervision, Funding acquisition. **Sébastien Jaquemet**: Investigation, Resources, Writing - Review & Editing, Funding acquisition. **Gauthier Schaal**: Conceptualization, Writing - Review & Editing. **Marina Renedo**: Writing - Review & Editing. **Lucien Besnard**: Writing - Review & Editing. **Yves Cherel**: Resources, Writing - Review & Editing. **David Point**: Resources, Writing - Review & Editing, Supervision, Funding acquisition.

Foraging depth

MIF

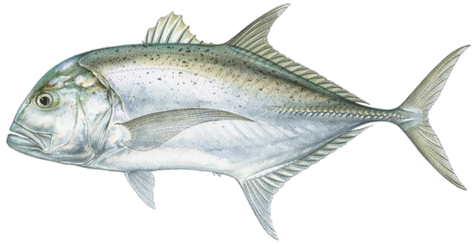

no MIF

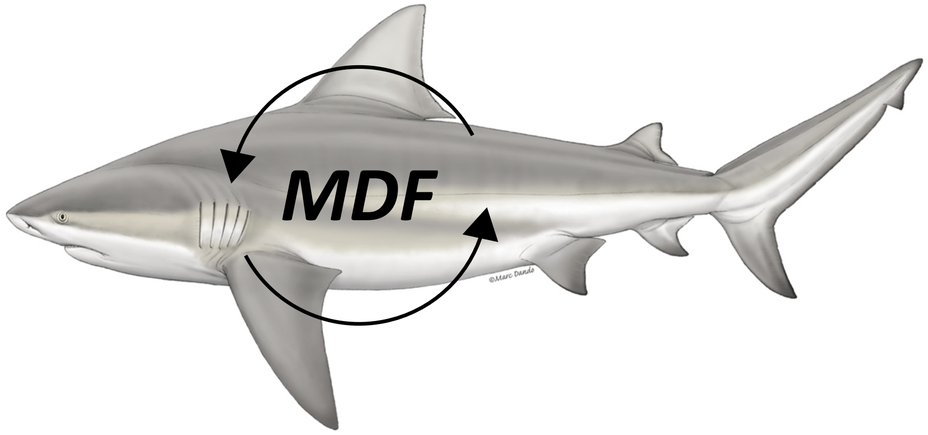

MeHg trophic transfer

MeHg demethylation

no MIF

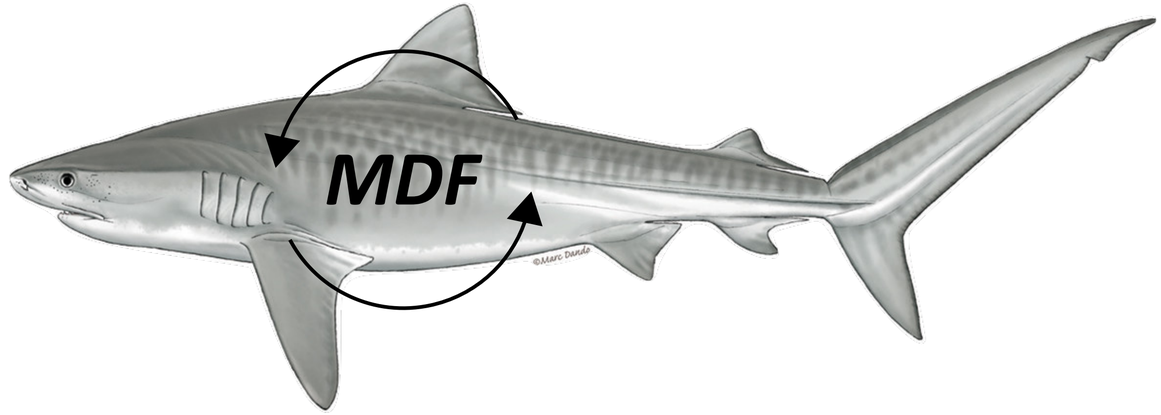

Mercury isotopes as tracers of ecology and metabolism in two sympatric shark species

Gaël Le Croizier[1*], Anne Lorrain[2], Jeroen E. Sonke[1], Sébastien Jaquemet[3], Gauthier Schaal[2], Marina Renedo[1], Lucien Besnard[2], Yves Cherel[4], David Point[1].

[1]Géosciences Environnement Toulouse (GET), Observatoire Midi Pyrénées (OMP), UMR 5563 CNRS/IRD/Université Paul Sabatier, 14 avenue Edouard Belin, 31400 Toulouse, France

[2]Laboratoire des Sciences de l'Environnement Marin (LEMAR), UMR 6539 CNRS/UBO/IRD/IFREMER, BP 70, 29280 Plouzané, France

[3]Laboratoire ENTROPIE, UMR 9220 CNRS/IRD/Université de La Réunion, 15 Avenue René Cassin, BP 92003, 97744 Saint-Denis, La Réunion, France

[4]Centre d'Etudes Biologiques de Chizé (CEBC), UMR 7372 du CNRS-La Rochelle Université, 79360 Villiers-en-Bois, France

ORCID numbers: 0000-0002-5093-8406 (G. Le Croizier), 0000-0001-7146-3035 (J. Sonke), 0000-0003-4199-4657 (S. Jaquemet), 0000-0003-3860-1517 (G. Schaal), 0000-0002-9224-8745 (M. Renedo), 0000-0001-9469-9489 (Y. Cherel), 0000-0002-1289-2072 (A. Lorrain), 0000-0002-5218-7781 (D. Point)

***Corresponding author**: gael.lecroizier@ird.fr

ABSTRACT

In coastal ecosystems, top predators are exposed to a wide variety of nutrient and contaminant sources due to the diversity of trophic webs within coastal areas. Mercury contamination could represent an additional threat to shark populations that are declining worldwide. Here we measured total mercury, carbon and nitrogen isotopes as well as mercury isotopes in two co-occurring shark species (the bull shark *Carcharhinus leucas* and the tiger shark *Galeocerdo cuvier*) and their prey from a coastal ecosystem of the western Indian Ocean (La Réunion Island), to (i) determine their main trophic Hg source and (ii) better characterize their diet composition and foraging habitat. Hg isotope signatures (Δ^{199}Hg and δ^{202}Hg) of shark prey suggested that bull sharks were exposed to methylmercury (MeHg) produced in the water column while tiger sharks were exposed to mesopelagic MeHg with additional microbial transformation in slope sediments. Δ^{199}Hg values efficiently traced the ecology of the two predators, demonstrating that bull sharks targeted coastal prey in shallow waters while tiger sharks were mainly foraging on mesopelagic species in the slope deeper waters. Unexpectedly, we found a positive shift in δ^{202}Hg (> 1‰) between sharks and their prey, leading to high δ^{202}Hg values in the two shark species (e.g. 1.91 ± 0.52 ‰ in the bull shark). This large shift in δ^{202}Hg indicates that sharks may display strong MeHg demethylation abilities, possibly reflecting evolutionary pathways for mitigating their MeHg contamination.

1. Introduction

Mercury (Hg) contamination constitutes a major global environmental concern, resulting in deleterious effects on marine organisms due to exposure to the toxic methylmercury (MeHg) form (Cáceres-Saez et al., 2018; Krey et al., 2015; Scheuhammer et al., 2015). Located at the interface between the atmosphere, lands, rivers and oceans, coastal areas are exposed to a wide variety of Hg sources and are at the same time used extensively and increasingly for a large number of activities, including resources exploitation or tourism. Within these complex ecosystems, long-lived organisms at the top of food webs usually display the highest Hg levels, due to bioaccumulation and biomagnification processes, which correspond to the increase of MeHg and other contaminant concentration over time and with the trophic position, respectively. Populations of marine predators are declining worldwide (Baum et al., 2003; Ferretti et al., 2008; Myers and Worm, 2003), including coastal sharks (Hammerschlag et al., 2019; Roff et al., 2018). The harmful effects of MeHg could thus represent an additional threat to the most depleted shark populations.

The bull shark *Carcharhinus leucas* and the tiger shark *Galeocerdo cuvier* are among the largest marine top-predators, playing a key role in tropical marine ecosystems (Roff et al., 2016). Due to their high trophic position and long life span, they are known to accumulate high MeHg levels (McKinney et al., 2016). The two species can be temporarily sympatric (i.e. co-occurring) in coastal ecosystems, but they also exhibit different habitat use involving incursions in freshwater and strong affinity for coral reefs for the bull shark (Espinoza et al., 2016; Matich and Heithaus, 2015; Werry et al., 2012) and large offshore movements for tiger sharks (James S. E. Lea et al., 2015; Meyer et al., 2018), during which they can dive in deep waters (Afonso and Hazin, 2015). Despite similar trophic positions, the

two species demonstrate segregation in their feeding habitats. While bull sharks can show high individual specialization and a strong dependence on coastal resources, tiger sharks are generalist predators able to rely on both coastal and oceanic prey (Dicken et al., 2017; Trystram et al., 2016).

Top predators using coastal ecosystems are known to feed on different food webs (Bird et al., 2018), inducing exposure to different sources and concentrations of contaminants (Le Croizier et al., 2016, 2019b). To characterize dietary resources, nitrogen and carbon stable isotopes ($\delta^{15}N$ and $\delta^{13}C$) are traditionally used in ecotoxicological studies (Le Bourg et al., 2019; Le Croizier et al., 2020), reflecting respectively the trophic position (Pethybridge et al., 2018) and foraging habitat (Bird et al., 2018) of consumers. However, these tools show limitations, such as the variability of N and C isotopic fractionation during trophic transfers (Kim et al., 2012; Malpica-Cruz et al., 2012). More recently, new techniques such as Hg stable isotope analyses have been applied to characterize the sources and transfer routes of this contaminant (Gehrke et al., 2011; Sackett et al., 2017; Senn et al., 2010).

In seawater, MeHg is subject to mass-independent fractionation ("MIF", generally represented by $\Delta^{199}Hg$) under the influence of solar radiation, which induces a preferential photochemical demethylation of the light and odd-mass isotopes. In the photic zone (i.e. the part of the water column exposed to light), the remaining MeHg pool available to marine organisms is therefore enriched in the heavy and odd-mass Hg isotopes. This process induces a $\Delta^{199}Hg$ gradient from the surface (photic or epipelagic zone, between 0 and 200 m deep) to depth (twilight or mesopelagic zone, between 200 and 1000 m deep), with higher $\Delta^{199}Hg$ values near the surface. This isotopic gradient allows to trace the vertical foraging habitat of

marine consumers (Blum et al., 2013; Madigan et al., 2018; Sackett et al., 2017). Moreover, Δ^{199}Hg constitutes a trophic tracer of major interest since Δ^{199}Hg values are conserved between prey and predators due to the absence of MIF during trophic interactions or metabolic processes (Kwon et al., 2016, 2012; Masbou et al., 2018).

Hg isotopes are also subject to mass-dependent fractionation ("MDF", generally represented by δ^{202}Hg) that takes place during physico-chemical processes such as photoreduction (Bergquist and Blum, 2007) and volatilization (Zheng et al., 2007), but also during biological processes such as methylation (Janssen et al., 2016) and demethylation (Perrot et al., 2016). δ^{202}Hg can be used to assess the Hg metabolism, such as the transformation of MeHg into less toxic inorganic Hg (iHg) by demethylation in the liver of marine organisms (Bolea-Fernandez et al., 2019). Indeed, the preferential demethylation of light Hg isotopes induces an increase in δ^{202}Hg in the remaining MeHg pool which is ultimately accumulated in other tissues such as muscle (Perrot et al., 2016). Thereby, significant enrichment of δ^{202}Hg is generally found in mammal muscle and human hair relative to trophic Hg sources, reflecting in vivo demethylation of MeHg (Laffont et al., 2011; Li et al., 2014; Perrot et al., 2012).

In the western Indian Ocean, only a few studies have documented Hg concentrations in coastal species (Le Bourg et al., 2019; Sardenne et al., 2017), with most studies focusing on offshore organisms (Bodin et al., 2017; Kiszka et al., 2015). In addition to trophic position and body length, foraging habitat was found to influence Hg levels in various shark species sampled across different locations in the southwestern Indian Ocean, including La Réunion Island (Le Bourg et al., 2019). Indeed, higher Hg concentrations were observed in offshore and deep-sea species compared to coastal species, suggesting different sources of MeHg

exposure between sharks feeding in nearshore shallow waters and those feeding in offshore deep waters (Kiszka et al., 2015; Le Bourg et al., 2019). On the other hand, high Hg concentrations were found in large coastal shark species from the east coast of South-Africa without apparent influence of foraging depth (McKinney et al., 2016). The role of feeding depth in MeHg exposure therefore remains to be clarified for predators using nearshore ecosystems in the western Indian Ocean. Moreover, while hepatic demethylation of MeHg is well known in marine mammals (Bolea-Fernandez et al., 2019; Perrot et al., 2016), bony fish do not appear to have such metabolic capacities. Although it has recently been suggested that sharks may have protective mechanisms that mitigate Hg toxicity (Merly et al., 2019), to date there is no evidence of MeHg demethylation in sharks.

In this context, the present study focused on two sympatric predator species, the bull and the tiger shark, sampled in a coastal ecosystem of the Indian Ocean (La Réunion Island). The two major objectives were to:

1) Use Hg MIF signatures (Δ^{199}Hg values) as diet and foraging depth tracers to determine whether different MeHg sources contribute to MeHg burdens in the two shark species.
2) Use Hg MDF signatures (δ^{202}Hg values) as tracers of Hg metabolism to evaluate the MeHg demethylation abilities in sharks.

2. Material and methods

2.1 Sampling

The study was carried out in the coastal ecosystem of La Réunion Island, an oceanic island located in the southwestern Indian Ocean. The island is of volcanic origin and its topography is characterized by abrupt slopes inducing close proximity between coastal and offshore ecosystems. This remote island is far from continental masses and therefore far from the main sources of industrial pollution.

Muscle samples from 20 bull sharks *Carcharhinus leucas* (10 males, 10 females) and 20 tiger sharks *Galeocerdo cuvier* (8 males, 12 females) were collected from individuals caught by local fishermen along the island slope on the west coast of La Réunion Island in 2015 (Figure 1). To minimize the impact of ontogenetic changes in diet and habitat on Hg isotope values, most of the sharks were sub-adults and adults (i.e. > 259 cm for tiger sharks (Werry et al., 2014) and > 160 cm for bull sharks (Werry et al., 2011) (SI Global dataset), and were thus larger than the size at which dietary shifts occur (i.e. 200-230 cm for tiger sharks and 140 cm for bull sharks) (Habegger et al., 2012; Lowe et al., 1996).

At La Réunion island, teleost fish species dominate the preys consumed by both bull and tiger sharks, based on stomach contents (i.e. respectively 93% and 78% in terms of mass percentage) (Trystram et al., 2016). However, the large diversity of prey (i.e. 56 and 148 species for bull and tiger sharks, respectively) (Trystram et al., 2016) makes it very difficult to cover the full prey spectrum of sharks. In this context, we collected muscle samples from fish with known ecology and representative of the different habitats that sharks could use for foraging and by which Hg exposure could occur (SI Table S3). In a similar coastal ecosystem (Hawaii, USA), terrestrial freshwater inputs to coastal sediments were previously identified as the primary source of tissue Hg in the giant trevally *Caranx ignobilis* (Sackett et al., 2017). In the present study, this fish species was then used as a proxy of Hg sources from the

demersal nearshore habitat. The yellow-edged lyretail *Variola louti*, a reef-associated grouper was sampled here to represent the shallow coral ecosystem (Emslie et al., 2017) while the great barracuda *Sphyraena barracuda* and the wahoo *Acanthocybium solandri* were collected to represent the epipelagic nearshore habitat (Trystram, 2016). The deepwater longtail red snapper *Etelis coruscans* was identified as primarily exposed to MeHg through deepwater sediments (Sackett et al., 2017) and was thus used as a proxy of MeHg sources from slope waters. Regarding pelagic offshore Hg sources, tuna species (i.e. the yellowfin tuna *Thunnus albacares* and the skipjack tuna *Katsuwonus pelamis*) and the lantern fish *Ceratoscopelus warmingii* were used as proxies of respectively epipelagic and mesopelagic Hg sources, according to their known ecology and previously published Hg isotope values (Blum et al., 2013; Madigan et al., 2018). *Ceratoscopelus warmingii* was collected during the "La Pérouse" and "MAD-RIDGE-1" scientific cruises in 2016 aboard the RV Antea off La Réunion Island and off southern Madagascar, respectively. All the other fish species were sampled between January 2012 and December 2014 off the west coast of La Réunion Island by local fishermen (Figure 1).

All samples were kept in a cool box following collection and thereafter frozen at –20 °C in the laboratory until further analysis. Muscle samples were freeze-dried and ground into a fine and homogeneous powder using an automated grinder.

2.2 Muscle $\delta^{13}C$ and $\delta^{15}N$ values

Urea and lipid extraction were not applied on shark samples. Although shark muscle generally contains low lipid content (<1%) (Meyer et al., 2017), lipids are depleted in ^{13}C and shark osmoregulatory strategy induce a significant urea retention which is depleted in ^{15}N. This may cause bias in the interpretation of the $\delta^{13}C$ and $\delta^{15}N$, and therefore requires a

mathematical normalization for the $\delta^{13}C$ and $\delta^{15}N$ values following urea and lipid extraction in several species of sharks (Y. Li et al., 2016). Here, we applied the normalization equations established for the bull and the tiger shark from La Réunion Island, for each species and each sex (Martin and Jaquemet, 2019).

Approximately 0.5 mg of muscle were weighed and packed into tin capsules. Isotopic composition (with a precision of 0.1‰ for both $\delta^{13}C$ and $\delta^{15}N$) and carbon percentage and nitrogen percentage content were measured at the Stable Isotope Laboratory, GNS Science, Lower Hutt, New Zealand, using an Isoprime isotope ratio mass spectrometer interfaced to an EuroEA elemental analyzer in continuous-flow mode (EA-IRMS). Results are expressed in standard δ notation based on international standards (Vienna Pee Dee Belemnite for $\delta^{13}C$ and atmospheric nitrogen for $\delta^{15}N$) following the equation $\delta^{13}C$ or $\delta^{15}N = [(Rsample / Rstandard) - 1] \times 10^3$ (in ‰), where R is $^{13}C/^{12}C$ or $^{15}N/^{14}N$.

2.3 Hg concentration and speciation

Total Hg (THg) determination was carried out on an aliquot (around 20 mg) of dried fish or shark muscle by combustion, gold trapping and atomic absorption spectrophotometry detection using a DMA80 analyzer (Milestone, USA). Mercury concentrations in muscle samples are expressed on a dry weight basis ($\mu g \cdot g^{-1}$ dw). Only one analysis was performed per sample, but the accuracy and reproducibility of the method were established using two freeze-dried certified biological materials: a tuna fish flesh homogenate reference material (IAEA 436, IRMM) and a lobster hepatopancreas reference material (TORT 3, NRCC). The certified values for IAEA 436 (4.19 ± 0.36 $\mu g \cdot g^{-1}$ dw) were reproduced (measured value: 4.20 ± 0.09 $\mu g \cdot g^{-1}$ dw, n=10) within the confidence limits. The certified values for TORT 3

(0.292 ± 0.022 µg·g^{-1} dw) were also reproduced (measured value: 0.286 ± 0.024 µg·g^{-1} dw, n=10) within the confidence limits. The detection limit was 0.005 µg·g^{-1} dw.

THg is known to be almost exclusively in the MeHg form in shark and fish muscle (Bosch et al., 2016; de Carvalho et al., 2014; Pethybridge et al., 2010; Ruiz-de-Cenzano et al., 2014), including species sampled in this study (e.g. giant trevally and deepwater snapper (Sackett et al., 2015), bull shark (Matulik et al., 2017)). However, a subset of muscle samples from 10 bull sharks were analyzed for MeHg, specifically to verify that MeHg accounted for the majority of THg in our shark muscle samples and to evaluate the link between δ^{202}Hg values and Hg speciation. We focused on the bull shark, which showed the highest δ^{202}Hg variability, and selected 5 individuals with the lowest δ^{202}Hg values and 5 sharks with the highest δ^{202}Hg values (SI Figure S3). MeHg concentrations in shark samples were obtained by the selective and quantitative extraction of MeHg followed by cold-vapor atomic fluorescence spectroscopy (CV-AFS) determinations according to the procedure described by (Masbou et al., 2013). MeHg fraction was expressed as the percentage of MeHg to THg ratio. A tuna fish flesh homogenate reference material (BCR 464, IRMM) was tested to ensure measurement accuracy and reproducibility, and a MeHg recovery of 95 ± 1% (n=2) was obtained relative to certified concentration.

2.4 Hg isotopes

Aliquots of approximately 20 mg of dry muscle were left over night at room temperature in 3 mL of concentrated bi-distilled nitric acid (HNO_3). Samples were then digested on a hotplate for 6h at 85°C in pyrolyzed glass vessels closed by Teflon caps. One mL of hydrogen peroxide (H_2O_2) was added and digestion was continued for another 6h at 85°C. One hundred µL of BrCl was then added to ensure a full oxidation of MeHg to inorganic

Hg. The digest mixtures were finally diluted in an inverse aqua regia (3 HNO3: 1 HCl, 20 vol.% MilliQ water) to reach a nominal Hg concentration of 1 $ng \cdot g^{-1}$. Three types of certified reference materials (TORT 3, BCR 464, IAEA 436) and blanks were prepared in the same way as tissue samples (SI Table S1).

Mercury isotope compositions were measured at the Observatoire Midi-Pyrenées using multicollector inductively coupled plasma mass spectrometry (MC–ICP–MS, Thermo Finnigan Neptune Plus) with continuous-flow cold vapor (CV) generation using Sn(II) reduction (CETAC HGX-200), according to a previously published method (Enrico et al., 2016; Goix et al., 2019; Masbou et al., 2015). Hg isotope composition is expressed in δ notation and reported in parts per thousand (‰) deviation from the NIST SRM 3133 standard, which was determined by sample-standard bracketing according to the following equation: $\delta^{XXX}Hg$ (‰) = [($(^{XXX}Hg/^{198}Hg)_{sample}$ / $(^{XXX}Hg/^{198}Hg)_{NIST\ 3133}$) -1] X 1000

where xxx represents the mass of each mercury isotope. ^{204}Hg was not measured due to limitations in MC-ICP-MS cup configuration. $\delta^{202}Hg$ is used as a measure of MDF. Measures of MIF are calculated as the difference between a measured δ-value, and the predicted δ-value that is calculated by multiplying the measured $\delta^{202}Hg$ value by the kinetic MDF fractionation factor for each isotope (Bergquist and Blum, 2007). MIF is expressed by the Δ notation:

$\Delta^{199}Hg$ (‰) = $\delta^{199}Hg$ – ($\delta^{202}Hg$ X 0.252)

$\Delta^{200}Hg$ (‰) = $\delta^{200}Hg$ – ($\delta^{202}Hg$ X 0.502)

$\Delta^{201}Hg$ (‰) = $\delta^{201}Hg$ – ($\delta^{202}Hg$ X 0.752)

Total Hg in the diluted digest mixtures was monitored by MC-ICP-MS using ^{202}Hg signals: mean recoveries of 95 ± 6% (n = 72) for samples and 93 ± 12% (n =10) for certified reference

materials were found, ensuring efficient digestion of samples. Hg levels in blanks were below the detection limit. Reproducibility of Hg isotope measurements was assessed by analyzing UM-Almadén (n = 13), ETH-Fluka (n = 12) and the biological tissue procedural standards NRC TORT-3, ERM-BCR-464, and IAEA-436 (n = 10) (SI Table S1). Only one analysis was performed per sample, but measured isotope signatures as well as analytical reproducibility of standards were found to be in agreement with previously published values (Blum et al., 2013; Jiskra et al., 2017; M. Li et al., 2016; Masbou et al., 2013).

2.5 Statistics

Data was first checked for normality (Shapiro–Wilks test) and homogeneity of variances (Bartlett test). When these conditions were met, one-way ANOVAs were performed to test for differences between groups, followed by Tukey's HSD tests when more than two groups were compared. Otherwise, non-parametric analogues were used, i.e. Kruskal–Wallis tests (KW), followed by Conover–Iman multiple comparison tests with Bonferroni's adjustment in the presence of several groups.

Depending on data distribution (Shapiro–Wilks test), Pearson or Spearman correlation tests were used to investigate the correlation between shark THg concentration and other variables (length, mass, $\delta^{15}N$ and $\delta^{13}C$).

Using $\delta^{13}C$ and $\delta^{15}N$ values, standard ellipse areas encompassing 95% of the data (SEA_B, Bayesian SEA) were used to quantify the niche width and overlap between the two shark species, using the “SIBER” package (Jackson et al., 2011). The SEA_B constitutes a proxy of the feeding niche occupied by one species while the overlap between SEA_B quantifies the trophic

competition between species. The SEA_B overlap is expressed as a proportion of the non-overlapping area of the two ellipses.

Linear regressions were used to assess the relationships between i) Hg metabolism (using $\delta^{202}Hg$ as a proxy for MeHg demethylation) and shark age (using length as a proxy for age) (Bolea-Fernandez et al., 2019), ii) Hg MIF ($\Delta^{199}Hg$) and Hg MIF ($\Delta^{201}Hg$) as an indicator of MeHg photodemethylation *versus* iHg photoreduction in seawater (Bergquist and Blum, 2007), iii) Hg MIF ($\Delta^{199}Hg$) and Hg MDF ($\delta^{202}Hg$) as an indicator of Hg photodegradation *versus* microbial transformation (Bergquist and Blum, 2007).

Mean values are expressed with one standard deviation (1SD) unless otherwise stated (2SD). All statistical analyses were performed using the open source software R (version 3.6.1, R Core Team, 2019).

3. Results

3.1 Comparison of the two shark species

Tiger sharks had higher length (ANOVA; $p < 0.001$) but similar body mass (KW; $p > 0.05$) than bull shark (SI Table S2). The bull shark showed significantly higher THg concentration (4148 ± 3069 $ng \cdot g^{-1}$) (KW; $p < 0.01$), as well as higher muscle $\delta^{15}N$ (14.22 ± 0.47 ‰) and $\delta^{13}C$ values (-16.00 ± 0.58 ‰) (ANOVA; $p < 0.001$) compared to the tiger shark (3186 ± 1252 $ng \cdot g^{-1}$, 13.27 ± 0.54 ‰, -17.01 ± 0.49 ‰ for THg, $\delta^{15}N$ and $\delta^{13}C$ values, respectively) (SI Table S2). THg was positively correlated with total length and body mass for both the bull (Pearson; $p < 0.001$) and the tiger shark (Spearman; $p < 0.05$). THg was not correlated with $\delta^{15}N$ or $\delta^{13}C$ values for either species. The two shark species showed similar

carbon and nitrogen isotopic niche area: 5.23 ‰² for the bull shark and 4.19 ‰² for the tiger shark (SEA_B with 95% credible interval), and a small area overlap of 18%. (SI Figure S1). Concerning Hg isotopes, muscle Δ^{199}Hg and Δ^{201}Hg values, as well as δ^{202}Hg values were significantly higher in bull sharks than in tiger sharks (Δ^{199}Hg and Δ^{201}Hg: ANOVA, $p < 0.001$; δ^{202}Hg: KW, $p < 0.001$) (SI Table S2). No difference was found between species for Δ^{200}Hg (0.08 ‰ and 0.06 ‰ for bull and tiger sharks respectively; ANOVA, $p > 0.05$). The two sharks showed similar variability in Δ^{199}Hg values (Bartlett test, $p > 0.05$) (Figure 2A), whereas bull sharks displayed higher variability for δ^{202}Hg values (from 1.04 to 2.82 ‰) compared to tiger sharks (from 0.74 to 1.7 ‰) (Bartlett test, $p < 0.001$) (Figure 2B). Δ^{199}Hg and δ^{202}Hg values were not correlated with δ^{15}N or δ^{13}C values for either species ($p > 0.05$). Δ^{199}Hg values were not correlated with body length in the two shark species ($p > 0.05$). A positive correlation was found between length and δ^{202}Hg values for the two species ($p < 0.001$; R^2=0.70 for the bull shark, and R^2=0.31 for the tiger shark) (Figures 3A and 3B), and between THg and δ^{202}Hg only for the bull shark ($p < 0.001$, SI Figure S2). MeHg accounted for 95 ± 8% of THg in the tiger shark and the MeHg fraction was not correlated with length nor δ^{202}Hg values (SI Figure S3).

3.2 Comparison between sharks and prey

Δ^{199}Hg in prey species exhibited a wide range of values, from 1.94‰ in the deepwater snapper to 2.72‰ in the lyretail grouper (SI Table S3 and Figure 2A). The bull shark displayed similar Δ^{199}Hg as the yellowfin tuna and the giant trevally, while the tiger shark shared similar Δ^{199}Hg with the deepwater snapper (ANOVA; $p > 0.05$) (Figure 2A). The two shark species showed different Δ^{199}Hg values from all the other prey species (*i.e.* lyretail grouper, wahoo, great barracuda, skipjack tuna, lantern fish) (ANOVA or KW; $p < 0.05$).

Muscle δ^{202}Hg in prey species ranged from 0.20‰ in the yellowfin tuna to 1.05‰ in the great barracuda (SI Table S3). The bull shark showed significantly higher δ^{202}Hg than all the prey species (ANOVA or KW; $p < 0.05$) (Figure 2B). δ^{202}Hg in the tiger shark was also higher than in most of the prey species (ANOVA; $p < 0.001$) except for the lyretail grouper and the great barracuda (ANOVA; $p < 0.05$).

3.3 Hg sources

The linear regression between Δ^{199}Hg and Δ^{201}Hg for the overall fish and shark samples displayed a slope of 1.23 ± 0.05 ($R^2 = 0.87$, $p < 0.001$) (SI Figure S4) while the linear regression between Δ^{199}Hg and δ^{202}Hg for teleost fish only displayed a slope of 0.64 ± 0.18 ($R^2 = 0.28$, $p < 0.01$) (SI Figure S5). The mesopelagic offshore lantern fish displayed similar Δ^{199}Hg and δ^{202}Hg values than the giant trevally, as well as similar Δ^{199}Hg but higher δ^{202}Hg than the deepwater snapper (SI Table S3). Compared to the previous study of Sackett *et al.*, 2017 in Hawaii (Sackett et al., 2017), significant higher δ^{202}Hg was found in the deepwater snapper in the present study (ANOVA, $p < 0.05$) (SI Table S4). Despite no significant difference in δ^{202}Hg and Δ^{199}Hg for the giant trevally between our study and Sackett *et al.*, 2017 (KW, $p > 0.05$), our values showed lower variance for both δ^{202}Hg and Δ^{199}Hg (Bartlett test, $p < 0.05$).

4. Discussion

4.1 Hg isotopes as tracers of shark ecology

- Foraging depth

According to the previously documented decrease in Δ^{199}Hg values with depth (Blum et al., 2013), the higher Δ^{199}Hg found in bull sharks is likely reflecting the use of shallower waters as main feeding habitat compared to tiger sharks, which would forage in deeper waters (Figure 2A). In previous studies in coastal environments, estuarine fish were characterized either by higher (M. Li et al., 2016) or lower MIF signature (Senn et al., 2010) than open ocean fish, depending on light penetration as a function of water turbidity. Except during episodes of heavy rain, the water clarity in the coastal ecosystem of La Réunion Island implies that Δ^{199}Hg values may possibly vary more over a vertical gradient (i.e. depending on depth) than a horizontal gradient (i.e. depending on the distance to the shore). This hypothesis is supported by the fact that epipelagic fish (i.e. living in the upper part of the water column) from the inshore (e.g. wahoo and great barracuda) and offshore habitat (e.g. skipjack and yellowfin tunas) did not differ in Δ^{199}Hg values (SI Table S3). Here, Δ^{199}Hg values fully corroborate what was previously observed by telemetry studies at this site, showing a higher presence of bull sharks in the coastal environment of La Réunion Island compared to tiger sharks (Blaison et al., 2015). Similarly, bull sharks showed a preferential use of shallow waters in the Indian Ocean when not migrating (usually less than 50 m with deepest dive at 164 m) (J. S. E. Lea et al., 2015), while tiger sharks have been recorded in oceanic waters down to more than 1000 m (Afonso and Hazin, 2015).

- Diet composition

Numerous studies have confirmed that Δ^{199}Hg values are conserved between prey and predators due to the absence of photochemical Hg MIF during trophic interactions or metabolic processes (Kwon et al., 2016, 2012; Masbou et al., 2018), which makes this tool a trophic tracer of major interest. At La Réunion Island, teleost fish species represent the large

majority of the prey consumed by both bull and tiger sharks, based on stomach contents (i.e. respectively 93% and 78% in terms of mass percentage) (Trystram et al., 2016). Carangid species such as the giant trevally constitute the most consumed family by bull sharks with more than 40% of the ingested mass, while tiger sharks are more generalist predators and target a large number of teleost families. Stable isotope tracers were in accordance with stomach contents, as the bull shark had similar Δ^{199}Hg values (Figure 2A) but higher δ^{15}N values (as a proxy for trophic position) than the giant trevally (δ^{15}N = 14.22 ‰ and 12.53 ‰ for bull sharks and giant trevally respectively; ANOVA, $p < 0.001$), supporting the idea that carangid species are common prey for bull sharks. Alternatively, the largest giant trevallies could also share the feeding habitat of bull sharks leading to competition for resources and similar Δ^{199}Hg values. Associations between the two species have indeed been observed by video and acoustic (Loiseau, unpublished data). On the other hand, taking into account that epipelagic fish from the inshore and offshore habitats did not differ in MIF values (SI Table S3), the Δ^{199}Hg overlap between the bull shark and yellowfin tuna may only reflect the use of the same water depth across different food webs (i.e. respectively inshore and offshore) rather than trophic interactions, since tuna species were not identified among bull shark prey at La Réunion Island (Trystram et al., 2016). This underlines the importance of considering the information given by stomach contents and trophic positions to interpret Δ^{199}Hg values, which are preserved throughout food webs. Here, the tiger shark and the deepwater snapper shared the same Δ^{199}Hg (Figure 2A) but different trophic positions (i.e. higher δ^{15}N for the tiger shark; ANOVA, $p < 0.001$). As this bottom-associated snapper is found in waters around 300 m depth (Trystram et al., 2015), it suggests that tiger sharks are primarily targeting prey on the island slope. The two different isotopic approaches used in this study (i.e. Δ^{199}Hg and δ^{15}N/δ^{13}C) both lead to the conclusion that the two shark species

occupy different trophic niches (different Δ^{199}Hg and small SEA_b overlap) (Figure 2A and S2) but also that their trophic niches are similar in size (similar variance for Δ^{199}Hg (Bartlett Test, $p < 0.05$) and similar SEA_b). In a previous study based on δ^{13}C and δ^{15}N values, a trophic independence of the epipelagic fish community (including both the bull and the tiger shark) and the mesopelagic fish community was observed (Trystram et al., 2015). Here, Hg isotopes confirm segregation between bull sharks and deep species such as the deepwater snapper, but in contrast, provide evidence that tiger sharks rely on mesopelagic resources.

Overall, these results highlight the interest of Hg isotopes to address fundamental ecological questions, such as habitat use and trophic energy transfers (Tsui et al., 2020).

4.2 Hg isotopes as tracers of shark metabolism

- Comparison between sharks and bony fish

While Δ^{199}Hg values in sharks were comparable to those of other fish species in this area (Figure 2A), δ^{202}Hg values were generally higher in sharks compared to their potential teleost prey (Figure 2B). More precisely, both shark species stand out from their prey by more than 1 ‰ in δ^{202}Hg while having similar Δ^{199}Hg values. To our knowledge, such high δ^{202}Hg values (i.e. 1.9 ‰ in the bull shark and 1.2 ‰ in the tiger shark) have never been reported in fish. However, similar high values have been documented in mammals, including humans, that are able to metabolize MeHg to inorganic Hg by demethylation in the liver (Laffont et al., 2011; Masbou et al., 2018, 2015; Perrot et al., 2016). The preferential demethylation of light Hg isotopes induces an increase in δ^{202}Hg in the remaining MeHg pool that is ultimately accumulated in other tissues such as muscle (Perrot et al., 2016). This increase in MeHg δ^{202}Hg following demethylation varies from about 0.3 ‰ in terrestrial

mammals (Ma et al., 2018; Masbou et al., 2018), to around 1 ‰ in aquatic mammals (Perrot et al., 2016, 2012) and around 2 ‰ in humans (Laffont et al., 2011, 2009). Previous studies on mercury speciation have concluded that MeHg demethylation can occur in fish liver and intestine (Gonzalez et al., 2005; Wang et al., 2017). However, experimental studies using Hg isotopes in fish muscle do not allow to draw clear conclusions, with either no change in MDF signature between Hg trophic source and consumer (Feng et al., 2015; Kwon et al., 2012), or a positive (+ 0.35 ‰) (Kwon et al., 2013) or a negative shift in δ^{202}Hg values (- 0.19 ‰) (Kwon et al., 2016). In our study, δ^{202}Hg values in sharks were well above fractionation values previously published in fish (e.g. + 1.4 ‰ between the bull shark and the giant trevally), with the bull shark having higher δ^{202}Hg than all teleost species analyzed. This study represents the first isotopic investigation of Hg metabolism in sharks and supports the existence of MeHg demethylation in these predators.

High THg concentrations (around 150 $\mu g \cdot L^{-1}$) were found in the blood plasma of South African white sharks *Carcharodon carcharias*, at levels considered as toxic in other vertebrates (Merly et al., 2019). Despite this contamination, no alteration of the body condition nor negative effects on health parameters were observed suggesting that sharks may have protective mechanisms that mitigate Hg toxicity. Demethylation in sharks could therefore represent a mechanism limiting the accumulation of MeHg and its toxic effects. Moreover, MeHg concentrations are generally much higher in muscle compared to other organs such liver, kidney and brain in shark species (Bergés-Tiznado et al., 2015; Nam et al., 2011), suggesting that muscle could represent a storage tissue less sensitive to MeHg toxicity in sharks.

- Hg metabolism over age

δ^{202}Hg values increased with length, a proxy for age, in the two shark species studied here (Figures 3A and 3B). Most of the sharks were sub-adults and adults, and larger than the size at which the ontogenetic change in habitat and diet occurs (Habegger et al., 2012; Lowe et al., 1996). Furthermore, in the two shark species, none of the trophic markers analyzed (δ^{13}C, δ^{15}N, Δ^{199}Hg) were correlated with size. δ^{13}C and δ^{15}N were also not correlated with δ^{202}Hg, which does not support the influence of ontogenetic diet changes on δ^{202}Hg values. On the other hand, an enhancement of the demethylation rate with age was recently identified in the long-finned pilot whale *Globicephala melas*, leading to the decrease of the MeHg fraction in the muscle of older whales (from 99% to 65%) (Bolea-Fernandez et al., 2019). Since MeHg has higher δ^{202}Hg values compared to inorganic Hg (iHg) (Perrot et al., 2016), the decrease in MeHg fraction alongside the increase in iHg fraction in pilot whales was accompanied by a drop in δ^{202}Hg values (around 1 ‰ decrease) (Bolea-Fernandez et al., 2019). In our bull shark samples, MeHg accounted for 95% of total Hg, which is consistent with previous studies on this species (Matulik et al., 2017) or on other sharks (de Carvalho et al., 2014; Nam et al., 2011; Pethybridge et al., 2010). Moreover, no correlation was found between MeHg fraction and δ^{202}Hg or shark length (SI Figure S3A and S3B). These results imply that the change in δ^{202}Hg with age in shark muscle is unlikely to be the result of a variation in Hg speciation (i.e. MeHg versus iHg fraction). We thus hypothesize that the increase in δ^{202}Hg values with length could reflect a higher extent of MeHg demethylation in the liver of older sharks, before preferential storage of the remaining MeHg over iHg in muscle. By contrast, the aging muscle in pilot whale may gradually favor the storage of iHg over MeHg (Bolea-Fernandez et al., 2019). Moreover, a positive correlation was also observed between the δ^{202}Hg values and THg (as a proxy for MeHg) concentration only in the bull shark muscle (SI Figure S2). Such a positive correlation between δ^{202}Hg and THg was

previously observed in teleost fish species and were attributed to the excretion of isotopically light Hg by fish during Hg bioaccumulation (Bergquist and Blum, 2007). In the present study, the shift in Hg MDF signatures between sharks and their prey (e.g. + 1.4 ‰ for δ^{202}Hg between the bull shark and the giant trevally) is well above the values attributed experimentally to excretion in teleost fish (e.g. + 0.35 ‰ between the amberjack *Seriola dumerili* compared to its food) (Kwon et al., 2013). However, preferential efflux of MeHg with light Hg isotopes over time, through urinary or biliary excretion (Le Croizier et al., 2019a, 2018), may also contribute to the increase in δ^{202}Hg values observed in shark muscle. In addition, as previously proposed in pilot whales (Bolea-Fernández et al., 2019), it is possible that muscle MeHg can be recycled to the liver and undergo additional demethylation. Thus, older sharks may have experienced more MeHg exchanges between liver and muscle, leading to higher δ^{202}Hg values in the remaining MeHg. This hypothesis would explain the increase in δ^{202}Hg with shark length and THg concentration which both increase with age, respectively due to growth and bioaccumulation.

According to length, the age of individual sharks is supposed to vary from around 5 years to more than 25 years for bull sharks (Natanson et al., 2014) and from around 2 years to more than 15 years for tiger sharks (Meyer et al., 2014). As bull sharks are on average older and display a broader year range between individuals, this could explain their higher δ^{202}Hg values and higher intraspecific variability compared to tiger sharks (Figure 2B), caused by an increase in demethylation and / or more liver-muscle exchanges over time.

4.3 Hg exposure sources to sharks

- Hg cycle in the shark environment

In open oceans, Hg inputs to the surface waters mainly occur through rainfall wet deposition of inorganic Hg (iHg) and atmospheric dissolution of gaseous Hg (Hg(0)) (Zhang et al., 2014). Although the processes responsible for the mass-independent fractionation of even Hg isotopes remain uncertain, Δ^{200}Hg is thought to result from high-altitude Hg photo-oxidation in the tropopause (Chen et al., 2012). iHg wet deposition is characterized by a Δ^{200}Hg between 0 and 0.3 ‰ while Δ^{200}Hg of atmospheric Hg(0) ranges from -0.11 to -0.01 ‰ (Enrico et al., 2016; Gratz et al., 2010). In the present study, Δ^{200}Hg values were similar between the two shark species (i.e. 0.08 ± 0.04 ‰ in the bull shark and 0.06 ± 0.04 ‰ in the tiger shark) (SI Table S2), implying that the iHg precursor to MeHg in sharks originates from a common source, which may correspond to a combination of rainfall iHg and gaseous Hg(0) (with positive and negative Δ^{200}Hg values, respectively). Although to our knowledge there is still no data on the isotopic signature of Hg(0) in this region, preliminary Δ^{200}Hg in rainwater collected at La Réunion Island is 0.12 ‰ (Araujo et al., unpublished data), which suggests that MeHg in sharks is mostly derived from the methylation of iHg from wet deposition to the marine ecosystem, as previously observed in other aquatic ecosystems (Lepak et al., 2018).

Under the action of solar radiation, dissolved MeHg will be transformed into iHg by photodemethylation, while dissolved iHg will be transformed into Hg(0) by photoreduction. Photodemethylation of MeHg is characterized by a Δ^{199}Hg/Δ^{201}Hg ratio of 1.36 while photodegradation of inorganic Hg leads to a ratio of 1.0 (Bergquist and Blum, 2007). In the present study, overall fish and shark values displayed a mean Δ^{199}Hg/Δ^{201}Hg ratio of 1.23 indicating the dominance of MeHg demethylation over iHg photoreduction. This ratio is

consistent with those previously reported in coastal and pelagic ecosystems of oceanic islands such as Hawaii (Blum et al., 2013; Sackett et al., 2017).

Experimental studies have shown that Hg photochemical degradation leads to an approximate $\Delta^{199}Hg/\delta^{202}Hg$ slope of 2.4 whereas microbial transformation (no MIF) is characterized by a slope of 0 (Bergquist and Blum, 2007). In our study, the Hg isotopic signatures of the teleost prey displayed a $\Delta^{199}Hg/\delta^{202}Hg$ slope of 0.64 (SI Figure S5), indicating the dominance of microbial transformation (i.e. methylation and/or demethylation) over photochemical degradation, which is similar to previous studies on Hawaiian marine bottomfish (Sackett et al., 2017) and coastal marine fish from the Gulf of Mexico (Senn et al., 2010).

- Hg isotope signatures in shark prey

The main trophic MeHg vector for the bull shark at La Réunion Island is thought to be constituted by nearshore fish such as the giant trevally (Trystram et al., 2015) which shared similar $\Delta^{199}Hg$ and $\delta^{202}Hg$ with offshore epipelagic species such as the skipjack tuna (SI Table S3, Figure 4). This result would suggest that MeHg to which bull sharks are exposed via trophic transfer originates from the offshore environment (Figure 4). This observation contrasts with the findings of a previous study in Hawaii where terrestrial freshwater inputs to coastal sediments were the primary MeHg source for the giant trevally (Sackett et al., 2017), resulting in higher inter-individual variability for both $\Delta^{199}Hg$ and $\delta^{202}Hg$ compared to our values (Bartlett test, $p < 0.05$; SI Table S4). This strengthens the hypothesis of a limited input of MeHg by freshwater runoff of estuarine waters into the coastal ecosystem of La Réunion Island. Rather, MeHg around La Reunion originates from methylation of iHg that is supplied by rainwater to the marine environment, as suggested by $\Delta^{200}Hg$ values.

According to Δ^{199}Hg values, mesopelagic species such as the deepwater snapper constitute the main vector of Hg trophic contamination for tiger sharks (Figure 2A). The deepwater snapper only shared similar Δ^{199}Hg with the lantern fish (SI Table S3, Figure 4). This is in full agreement with stomach content observations, which revealed that mesopelagic teleosts and especially lantern fish are the major prey of the deepwater snapper, accounting for around 60% of the total prey abundance (Trystram, 2016). In Hawaii, Hg isotopic signatures of bottom fish including deepwater snappers revealed the incorporation of mesopelagic offshore MeHg sources into the slope sediments, where MeHg was subject to additional negative MDF (due to microbial methylation and/or demethylation) before transfer to the marine consumers (Sackett et al., 2017). Here, a lower δ^{202}Hg was similarly found in the deepwater snapper compared to the lantern fish (SI Table S3, Figure 4). We thus suggest that the decrease in δ^{202}Hg between the mesopelagic source and the deepwater snapper is related to its partial consumption of benthic prey (around 20% of the total prey abundance) (Trystram, 2016) and consequent exposure to a MeHg pool having undergone microbial MDF (i.e. methylation and/or demethylation) in sediments (Figure 4). The consumption of benthic prey could also have exposed the deepwater snapper to another source of MeHg produced in the sediments and characterized by a lower δ^{202}Hg values than mesopelagic MeHg.

As previously observed for marine fish species in the central Pacific (Blum et al., 2013; Sackett et al., 2017), both bull and tiger sharks were exposed to two different MeHg pools derived from the same main source of oceanic origin, produced from deposited atmospheric iHg. The bull shark was exposed to epipelagic offshore MeHg, which was dietary transferred to the epipelagic nearshore habitat (Figure 4). On the other hand, the tiger shark was

519 exposed to a mixed pool of (i) mesopelagic offshore MeHg and (ii) benthic MeHg subject to
520 bacterial transformation in sediments.

521

522 5. Conclusion

523 Hg MIF signatures allowed to characterize the vertical feeding habitat of sharks, revealing
524 that bull sharks forage in shallow water while tiger sharks use deeper habitat on the island
525 slope. Our study highlights the potential of Δ^{199}Hg values for tracing the ecology of marine
526 species and brings important new perspectives on the habitat use of coastal predators in a
527 context of increasing human-shark interactions. Using Hg MDF signatures, our results also
528 revealed for the first time the capacity of sharks to breakdown MeHg via demethylation. This
529 may limit MeHg concentrations in these vulnerable species, among the most contaminated
530 in the animal kingdom.

531

532 **Acknowledgments:**

533 Gaël Le Croizier was supported by a postdoctoral grant from the French National Research
534 Institute for Sustainable Development (IRD). This work was financially supported by the
535 French National Research Agency project ANR-17-CE34-0010 MERTOX. Shark samples were
536 collected as part of the Charc (Feder Fund convention 2011 Presage N°33021) and Ecoreco-
537 Run (DEAL-Réunion BOP113) projects, fish samples were collected during DIPPLO (FEP,
538 Regional council and TCO funds), ANCRE-DMX2 (FEP fund N°40055/DMSOI/2013), La
539 Pérouse cruise (DOI: 10.17600/16004500) and MAD-RIDGE-2 cruise (DOI:
540 10.17600/16004900). C. Trystram contributed to the data collection and laboratory

processes at GNS Sciences under the supervision of K. Rogers. We thank Laure Laffont and Jérôme Chmeleff for expert management of the OMP mercury and mass spectrometry facilities. We finally thank Marc Dando for allowing us to use his shark illustrations.

REFERENCES

Afonso, A.S., Hazin, F.H.V., 2015. Vertical Movement Patterns and Ontogenetic Niche Expansion in the Tiger Shark, Galeocerdo cuvier. PLOS ONE 10, e0116720. https://doi.org/10.1371/journal.pone.0116720

Baum, J.K., Myers, R.A., Kehler, D.G., Worm, B., Harley, S.J., Doherty, P.A., 2003. Collapse and Conservation of Shark Populations in the Northwest Atlantic. Science 299, 389–392. https://doi.org/10.1126/science.1079777

Bergquist, B.A., Blum, J.D., 2007. Mass-Dependent and -Independent Fractionation of Hg Isotopes by Photoreduction in Aquatic Systems. Science 318, 417–420. https://doi.org/10.1126/science.1148050

Bird, C.S., Veríssimo, A., Magozzi, S., Abrantes, K.G., Aguilar, A., Al-Reasi, H., Barnett, A., Bethea, D.M., Biais, G., Borrell, A., Bouchoucha, M., Boyle, M., Brooks, E.J., Brunnschweiler, J., Bustamante, P., Carlisle, A., Catarino, D., Caut, S., Cherel, Y., Chouvelon, T., Churchill, D., Ciancio, J., Claes, J., Colaço, A., Courtney, D.L., Cresson, P., Daly, R., Necker, L. de, Endo, T., Figueiredo, I., Frisch, A.J., Hansen, J.H., Heithaus, M., Hussey, N.E., Iitembu, J., Juanes, F., Kinney, M.J., Kiszka, J.J., Klarian, S.A., Kopp, D., Leaf, R., Li, Y., Lorrain, A., Madigan, D.J., Maljković, A., Malpica-Cruz, L., Matich, P., Meekan, M.G., Ménard, F., Menezes, G.M., Munroe, S.E.M., Newman, M.C., Papastamatiou, Y.P., Pethybridge, H., Plumlee, J.D., Polo-Silva, C., Quaeck-Davies, K., Raoult, V., Reum, J., Torres-Rojas, Y.E., Shiffman, D.S., Shipley, O.N., Speed, C.W., Staudinger, M.D., Teffer, A.K., Tilley, A., Valls, M., Vaudo, J.J., Wai, T.-C., Wells, R.J.D., Wyatt, A.S.J., Yool, A., Trueman, C.N., 2018. A global perspective on the trophic geography of sharks. Nature Ecology & Evolution 2, 299–305. https://doi.org/10.1038/s41559-017-0432-z

Blaison, A., Jaquemet, S., Guyomard, D., Vangrevelynghe, G., Gazzo, T., Cliff, G., Cotel, P., Soria, M., 2015. Seasonal variability of bull and tiger shark presence on the west coast of Reunion Island, western Indian Ocean. African Journal of Marine Science 37, 199–208. https://doi.org/10.2989/1814232X.2015.1050453

Blum, J.D., Popp, B.N., Drazen, J.C., Anela Choy, C., Johnson, M.W., 2013. Methylmercury production below the mixed layer in the North Pacific Ocean. Nature Geosci 6, 879–884. https://doi.org/10.1038/ngeo1918

Bodin, N., Lesperance, D., Albert, R., Hollanda, S., Michaud, P., Degroote, M., Churlaud, C., Bustamante, P., 2017. Trace elements in oceanic pelagic communities in the western Indian Ocean. Chemosphere 174, 354–362. https://doi.org/10.1016/j.chemosphere.2017.01.099

Bolea-Fernández, E., Rua-Ibarz, A., Krupp, E., Feldmann, J., Vanhaecke, F., 2019. High-precision isotopic analysis sheds new light on mercury metabolism in long-finned pilot whales (Globicephala melas). Scientific Reports 9. https://doi.org/10.1038/s41598-019-43825-z

Bolea-Fernandez, E., Rua-Ibarz, A., Krupp, E.M., Feldmann, J., Vanhaecke, F., 2019. High-precision isotopic analysis sheds new light on mercury metabolism in long-finned pilot whales (Globicephala melas). Scientific Reports 9, 7262. https://doi.org/10.1038/s41598-019-43825-z

Bosch, A.C., O'Neill, B., Sigge, G.O., Kerwath, S.E., Hoffman, L.C., 2016. Heavy metal accumulation and toxicity in smoothhound (Mustelus mustelus) shark from Langebaan Lagoon, South Africa. Food Chemistry 190, 871–878. https://doi.org/10.1016/j.foodchem.2015.06.034

Cáceres-Saez, I., Haro, D., Blank, O., Aguayo Lobo, A., Dougnac, C., Arredondo, C., Cappozzo, H.L., Guevara, S.R., 2018. High status of mercury and selenium in false killer whales (Pseudorca crassidens, Owen 1846) stranded on Southern South America: A possible toxicological concern? Chemosphere 199, 637–646. https://doi.org/10.1016/j.chemosphere.2018.02.046

592 Chen, J., Hintelmann, H., Feng, X., Dimock, B., 2012. Unusual fractionation of both odd and even
593 mercury isotopes in precipitation from Peterborough, ON, Canada. Geochimica et
594 Cosmochimica Acta 90, 33–46. https://doi.org/10.1016/j.gca.2012.05.005
595 de Carvalho, G.G.A., Degaspari, I.A.M., Branco, V., Canário, J., de Amorim, A.F., Kennedy, V.H.,
596 Ferreira, J.R., 2014. Assessment of Total and Organic Mercury Levels in Blue Sharks (Prionace
597 glauca) from the South and Southeastern Brazilian Coast. Biol Trace Elem Res 159, 128–134.
598 https://doi.org/10.1007/s12011-014-9995-6
599 Dicken, M.L., Hussey, N.E., Christiansen, H.M., Smale, M.J., Nkabi, N., Cliff, G., Wintner, S.P., 2017.
600 Diet and trophic ecology of the tiger shark (Galeocerdo cuvier) from South African waters.
601 PLOS ONE 12, e0177897. https://doi.org/10.1371/journal.pone.0177897
602 Emslie, M.J., Cheal, A.J., Logan, M., 2017. The distribution and abundance of reef-associated
603 predatory fishes on the Great Barrier Reef. Coral Reefs 36, 829–846.
604 https://doi.org/10.1007/s00338-017-1573-x
605 Enrico, M., Roux, G.L., Marusczak, N., Heimbürger, L.-E., Claustres, A., Fu, X., Sun, R., Sonke, J.E.,
606 2016. Atmospheric Mercury Transfer to Peat Bogs Dominated by Gaseous Elemental Mercury
607 Dry Deposition. Environ. Sci. Technol. 50, 2405–2412.
608 https://doi.org/10.1021/acs.est.5b06058
609 Espinoza, M., Heupel, M.R., Tobin, A.J., Simpfendorfer, C.A., 2016. Evidence of Partial Migration in a
610 Large Coastal Predator: Opportunistic Foraging and Reproduction as Key Drivers? PLOS ONE
611 11, e0147608. https://doi.org/10.1371/journal.pone.0147608
612 Feng, C., Pedrero, Z., Gentès, S., Barre, J., Renedo, M., Tessier, E., Berail, S., Maury-Brachet, R.,
613 Mesmer-Dudons, N., Baudrimont, M., Legeay, A., Maurice, L., Gonzalez, P., Amouroux, D.,
614 2015. Specific Pathways of Dietary Methylmercury and Inorganic Mercury Determined by
615 Mercury Speciation and Isotopic Composition in Zebrafish (Danio rerio). Environ. Sci. Technol.
616 49, 12984–12993. https://doi.org/10.1021/acs.est.5b03587
617 Ferretti, F., Myers, R.A., Serena, F., Lotze, H.K., 2008. Loss of Large Predatory Sharks from the
618 Mediterranean Sea. Conservation Biology 22, 952–964. https://doi.org/10.1111/j.1523-
619 1739.2008.00938.x
620 Gehrke, G.E., Blum, J.D., Slotton, D.G., Greenfield, B.K., 2011. Mercury Isotopes Link Mercury in San
621 Francisco Bay Forage Fish to Surface Sediments. Environ. Sci. Technol. 45, 1264–1270.
622 https://doi.org/10.1021/es103053y
623 Goix, S., Maurice, L., Laffont, L., Rinaldo, R., Lagane, C., Chmeleff, J., Menges, J., Heimbürger, L.-E.,
624 Maury-Brachet, R., Sonke, J.E., 2019. Quantifying the impacts of artisanal gold mining on a
625 tropical river system using mercury isotopes. Chemosphere 219, 684–694.
626 https://doi.org/10.1016/j.chemosphere.2018.12.036
627 Gonzalez, P., Dominique, Y., Massabuau, J.C., Boudou, A., Bourdineaud, J.P., 2005. Comparative
628 Effects of Dietary Methylmercury on Gene Expression in Liver, Skeletal Muscle, and Brain of
629 the Zebrafish (Danio rerio). Environ. Sci. Technol. 39, 3972–3980.
630 https://doi.org/10.1021/es0483490
631 Gratz, L.E., Keeler, G.J., Blum, J.D., Sherman, L.S., 2010. Isotopic Composition and Fractionation of
632 Mercury in Great Lakes Precipitation and Ambient Air. Environ. Sci. Technol. 44, 7764–7770.
633 https://doi.org/10.1021/es100383w
634 Habegger, M.L., Motta, P.J., Huber, D.R., Dean, M.N., 2012. Feeding biomechanics and theoretical
635 calculations of bite force in bull sharks (Carcharhinus leucas) during ontogeny. Zoology 115,
636 354–364. https://doi.org/10.1016/j.zool.2012.04.007
637 Hammerschlag, N., Williams, L., Fallows, M., Fallows, C., 2019. Disappearance of white sharks leads to
638 the novel emergence of an allopatric apex predator, the sevengill shark. Scientific Reports 9,
639 1908. https://doi.org/10.1038/s41598-018-37576-6
640 Jackson, A.L., Inger, R., Parnell, A.C., Bearhop, S., 2011. Comparing isotopic niche widths among and
641 within communities: SIBER – Stable Isotope Bayesian Ellipses in R. Journal of Animal Ecology
642 80, 595–602. https://doi.org/10.1111/j.1365-2656.2011.01806.x

643 Janssen, S.E., Schaefer, J.K., Barkay, T., Reinfelder, J.R., 2016. Fractionation of Mercury Stable
644 Isotopes during Microbial Methylmercury Production by Iron- and Sulfate-Reducing Bacteria.
645 Environ. Sci. Technol. 50, 8077–8083. https://doi.org/10.1021/acs.est.6b00854
646 Jiskra, M., G. Wiederhold, J., Skyllberg, U., Kronberg, R.-M., Kretzschmar, R., 2017. Source tracing of
647 natural organic matter bound mercury in boreal forest runoff with mercury stable isotopes.
648 Environmental Science: Processes & Impacts 19, 1235–1248.
649 https://doi.org/10.1039/C7EM00245A
650 Kim, S.L., del Rio, C.M., Casper, D., Koch, P.L., 2012. Isotopic incorporation rates for shark tissues
651 from a long-term captive feeding study. J. Exp. Biol. 215, 2495–2500.
652 https://doi.org/10.1242/jeb.070656
653 Kiszka, J.J., Aubail, A., Hussey, N.E., Heithaus, M.R., Caurant, F., Bustamante, P., 2015. Plasticity of
654 trophic interactions among sharks from the oceanic south-western Indian Ocean revealed by
655 stable isotope and mercury analyses. Deep Sea Research Part I: Oceanographic Research
656 Papers 96, 49–58. https://doi.org/10.1016/j.dsr.2014.11.006
657 Krey, A., Ostertag, S.K., Chan, H.M., 2015. Assessment of neurotoxic effects of mercury in beluga
658 whales (Delphinapterus leucas), ringed seals (Pusa hispida), and polar bears (Ursus
659 maritimus) from the Canadian Arctic. Science of The Total Environment, Special Issue:
660 Mercury in Canada's North 509–510, 237–247.
661 https://doi.org/10.1016/j.scitotenv.2014.05.134
662 Kwon, S.Y., Blum, J.D., Carvan, M.J., Basu, N., Head, J.A., Madenjian, C.P., David, S.R., 2012. Absence
663 of fractionation of mercury isotopes during trophic transfer of methylmercury to freshwater
664 fish in captivity. Environmental science & technology 46, 7527.
665 https://doi.org/10.1021/es300794q
666 Kwon, S.Y., Blum, J.D., Chirby, M.A., Chesney, E.J., 2013. Application of mercury isotopes for tracing
667 trophic transfer and internal distribution of mercury in marine fish feeding experiments.
668 Environ. Toxicol. Chem. 32, 2322–2330. https://doi.org/10.1002/etc.2313
669 Kwon, S.Y., Blum, J.D., Madigan, D.J., Block, B.A., Popp, B.N., 2016. Quantifying mercury isotope
670 dynamics in captive Pacific bluefin tuna (*Thunnus orientalis*). Elem Sci Anth 4.
671 https://doi.org/10.12952/journal.elementa.000088
672 Laffont, L., Sonke, J.E., Maurice, L., Hintelmann, H., Pouilly, M., Sánchez Bacarreza, Y., Perez, T.,
673 Behra, P., 2009. Anomalous Mercury Isotopic Compositions of Fish and Human Hair in the
674 Bolivian Amazon. Environ. Sci. Technol. 43, 8985–8990. https://doi.org/10.1021/es9019518
675 Laffont, L., Sonke, J.E., Maurice, L., Monrroy, S.L., Chincheros, J., Amouroux, D., Behra, P., 2011. Hg
676 Speciation and Stable Isotope Signatures in Human Hair As a Tracer for Dietary and
677 Occupational Exposure to Mercury. Environmental Science & Technology 45, 9910–9916.
678 https://doi.org/10.1021/es202353m
679 Le Bourg, B., Kiszka, J.J., Bustamante, P., Heithaus, M.R., Jaquemet, S., Humber, F., 2019. Effect of
680 body length, trophic position and habitat use on mercury concentrations of sharks from
681 contrasted ecosystems in the southwestern Indian Ocean. Environmental Research 169, 387–
682 395. https://doi.org/10.1016/j.envres.2018.11.024
683 Le Croizier, G., Lacroix, C., Artigaud, S., Le Floch, S., Munaron, J.-M., Raffray, J., Penicaud, V., Rouget,
684 M.-L., Laë, R., Tito De Morais, L., 2019a. Metal subcellular partitioning determines excretion
685 pathways and sensitivity to cadmium toxicity in two marine fish species. Chemosphere 217,
686 754–762. https://doi.org/10.1016/j.chemosphere.2018.10.212
687 Le Croizier, G., Lacroix, C., Artigaud, S., Le Floch, S., Raffray, J., Penicaud, V., Coquillé, V., Autier, J.,
688 Rouget, M.-L., Le Bayon, N., Laë, R., Tito De Morais, L., 2018. Significance of metallothioneins
689 in differential cadmium accumulation kinetics between two marine fish species.
690 Environmental Pollution 236, 462–476. https://doi.org/10.1016/j.envpol.2018.01.002
691 Le Croizier, G., Lorrain, A., Schaal, G., Ketchum, J., Hoyos-Padilla, M., Besnard, L., Jean-Marie-
692 Munaron, Le Loc'h, F., Point, D., 2020. Trophic resources and mercury exposure of two

693 silvertip shark populations in the northeast Pacific Ocean. Chemosphere 126645.
694 https://doi.org/10.1016/j.chemosphere.2020.126645
695 Le Croizier, G., Schaal, G., Gallon, R., Fall, M., Le Grand, F., Munaron, J.-M., Rouget, M.-L., Machu, E.,
696 Le Loc'h, F., Laë, R., De Morais, L.T., 2016. Trophic ecology influence on metal
697 bioaccumulation in marine fish: Inference from stable isotope and fatty acid analyses.
698 Science of The Total Environment 573, 83–95.
699 https://doi.org/10.1016/j.scitotenv.2016.08.035
700 Le Croizier, G., Schaal, G., Point, D., Le Loc'h, F., Machu, E., Fall, M., Munaron, J.-M., Boyé, A., Walter,
701 P., Laë, R., Tito De Morais, L., 2019b. Stable isotope analyses revealed the influence of
702 foraging habitat on mercury accumulation in tropical coastal marine fish. Science of The Total
703 Environment 650, 2129–2140. https://doi.org/10.1016/j.scitotenv.2018.09.330
704 Lea, J. S. E., Humphries, N.E., Clarke, C.R., Sims, D.W., 2015. To Madagascar and back: long-distance,
705 return migration across open ocean by a pregnant female bull shark Carcharhinus leucas.
706 Journal of Fish Biology 87, 1313–1321. https://doi.org/10.1111/jfb.12805
707 Lea, James S. E., Wetherbee, B.M., Queiroz, N., Burnie, N., Aming, C., Sousa, L.L., Mucientes, G.R.,
708 Humphries, N.E., Harvey, G.M., Sims, D.W., Shivji, M.S., 2015. Repeated, long-distance
709 migrations by a philopatric predator targeting highly contrasting ecosystems. Scientific
710 Reports 5, 11202. https://doi.org/10.1038/srep11202
711 Lepak, R.F., Janssen, S.E., Yin, R., Krabbenhoft, D.P., Ogorek, J.M., DeWild, J.F., Tate, M.T., Holsen,
712 T.M., Hurley, J.P., 2018. Factors Affecting Mercury Stable Isotopic Distribution in Piscivorous
713 Fish of the Laurentian Great Lakes. Environ. Sci. Technol. 52, 2768–2776.
714 https://doi.org/10.1021/acs.est.7b06120
715 Li, M., Schartup, A.T., Valberg, A.P., Ewald, J.D., Krabbenhoft, D.P., Yin, R., Balcom, P.H., Sunderland,
716 E.M., 2016. Environmental Origins of Methylmercury Accumulated in Subarctic Estuarine Fish
717 Indicated by Mercury Stable Isotopes. Environ. Sci. Technol. 50, 11559–11568.
718 https://doi.org/10.1021/acs.est.6b03206
719 Li, M., Sherman, L.S., Blum, J.D., Grandjean, P., Mikkelsen, B., Weihe, P., Sunderland, E.M., Shine, J.P.,
720 2014. Assessing Sources of Human Methylmercury Exposure Using Stable Mercury Isotopes.
721 Environ. Sci. Technol. 48, 8800–8806. https://doi.org/10.1021/es500340r
722 Li, Y., Zhang, Y., Hussey, N.E., Dai, X., 2016. Urea and lipid extraction treatment effects on δ15N and
723 δ13C values in pelagic sharks. Rapid Communications in Mass Spectrometry 30, 1–8.
724 https://doi.org/10.1002/rcm.7396
725 Lowe, C.G., Wetherbee, B.M., Crow, G.L., Tester, A.L., 1996. Ontogenetic dietary shifts and feeding
726 behavior of the tiger shark, Galeocerdo cuvier, in Hawaiian waters. Environ Biol Fish 47, 203–
727 211. https://doi.org/10.1007/BF00005044
728 Ma, L., Evans, R.D., Wang, W., Georg, R.B., 2018. In vivo fractionation of mercury isotopes in tissues
729 of a mammalian carnivore (Neovison vison). Science of The Total Environment 627, 1228–
730 1233. https://doi.org/10.1016/j.scitotenv.2018.01.296
731 Madigan, D.J., Li, M., Yin, R., Baumann, H., Snodgrass, O.E., Dewar, H., Krabbenhoft, D.P., Baumann,
732 Z., Fisher, N.S., Balcom, P., Sunderland, E.M., 2018. Mercury Stable Isotopes Reveal Influence
733 of Foraging Depth on Mercury Concentrations and Growth in Pacific Bluefin Tuna. Environ.
734 Sci. Technol. 52, 6256–6264. https://doi.org/10.1021/acs.est.7b06429
735 Malpica-Cruz, L., Herzka, S.Z., Sosa-Nishizaki, O., Lazo, J.P., 2012. Tissue-specific isotope trophic
736 discrimination factors and turnover rates in a marine elasmobranch: empirical and modeling
737 results. Can. J. Fish. Aquat. Sci. 69, 551–564. https://doi.org/10.1139/f2011-172
738 Martin, U.M., Jaquemet, S., 2019. Effects of urea and lipid removal from Carcharhinus leucas and
739 Galeocerdo cuvier white muscle on carbon and nitrogen stable isotope ratios. Western
740 Indian Ocean Journal of Marine Science 18, 47-56–56.
741 Masbou, J., Point, D., Sonke, J.E., 2013. Application of a selective extraction method for
742 methylmercury compound specific stable isotope analysis (MeHg-CSIA) in biological
743 materials. J. Anal. At. Spectrom. 28, 1620–1628. https://doi.org/10.1039/C3JA50185J

744 Masbou, J., Point, D., Sonke, J.E., Frappart, F., Perrot, V., Amouroux, D., Richard, P., Becker, P.R.,
745 2015. Hg Stable Isotope Time Trend in Ringed Seals Registers Decreasing Sea Ice Cover in the
746 Alaskan Arctic. Environ. Sci. Technol. 49, 8977–8985. https://doi.org/10.1021/es5048446
747 Masbou, J., Sonke, J.E., Amouroux, D., Guillou, G., Becker, P.R., Point, D., 2018. Hg-Stable Isotope
748 Variations in Marine Top Predators of the Western Arctic Ocean. ACS Earth Space Chem.
749 https://doi.org/10.1021/acsearthspacechem.8b00017
750 Matich, P., Heithaus, M.R., 2015. Individual variation in ontogenetic niche shifts in habitat use and
751 movement patterns of a large estuarine predator (Carcharhinus leucas). Oecologia 178, 347–
752 359. https://doi.org/10.1007/s00442-015-3253-2
753 Matulik, A.G., Kerstetter, D.W., Hammerschlag, N., Divoll, T., Hammerschmidt, C.R., Evers, D.C., 2017.
754 Bioaccumulation and biomagnification of mercury and methylmercury in four sympatric
755 coastal sharks in a protected subtropical lagoon. Marine Pollution Bulletin 116, 357–364.
756 https://doi.org/10.1016/j.marpolbul.2017.01.033
757 McKinney, M.A., Dean, K., Hussey, N.E., Cliff, G., Wintner, S.P., Dudley, S.F.J., Zungu, M.P., Fisk, A.T.,
758 2016. Global versus local causes and health implications of high mercury concentrations in
759 sharks from the east coast of South Africa. Science of The Total Environment 541, 176–183.
760 https://doi.org/10.1016/j.scitotenv.2015.09.074
761 Merly, L., Lange, L., Meÿer, M., Hewitt, A.M., Koen, P., Fischer, C., Muller, J., Schilack, V., Wentzel, M.,
762 Hammerschlag, N., 2019. Blood plasma levels of heavy metals and trace elements in white
763 sharks (Carcharodon carcharias) and potential health consequences. Marine Pollution
764 Bulletin 142, 85–92. https://doi.org/10.1016/j.marpolbul.2019.03.018
765 Meyer, C.G., Anderson, J.M., Coffey, D.M., Hutchinson, M.R., Royer, M.A., Holland, K.N., 2018.
766 Habitat geography around Hawaii's oceanic islands influences tiger shark (Galeocerdo cuvier
767) spatial behaviour and shark bite risk at ocean recreation sites. Scientific Reports 8, 4945.
768 https://doi.org/10.1038/s41598-018-23006-0
769 Meyer, C.G., O'Malley, J.M., Papastamatiou, Y.P., Dale, J.J., Hutchinson, M.R., Anderson, J.M., Royer,
770 M.A., Holland, K.N., 2014. Growth and Maximum Size of Tiger Sharks (Galeocerdo cuvier) in
771 Hawaii. PLoS ONE 9, e84799. https://doi.org/10.1371/journal.pone.0084799
772 Meyer, L., Pethybridge, H., Nichols, P.D., Beckmann, C., Bruce, B.D., Werry, J.M., Huveneers, C., 2017.
773 Assessing the Functional Limitations of Lipids and Fatty Acids for Diet Determination: The
774 Importance of Tissue Type, Quantity, and Quality. Front. Mar. Sci. 4.
775 https://doi.org/10.3389/fmars.2017.00369
776 Myers, R.A., Worm, B., 2003. Rapid worldwide depletion of predatory fish communities. Nature 423,
777 280–283. https://doi.org/10.1038/nature01610
778 Nam, D.-H., Adams, D.H., Reyier, E.A., Basu, N., 2011. Mercury and selenium levels in lemon sharks
779 (Negaprion brevirostris) in relation to a harmful red tide event. Environ Monit Assess 176,
780 549–559. https://doi.org/10.1007/s10661-010-1603-4
781 Natanson, L.J., Adams, D.H., Winton, M.V., Maurer, J.R., 2014. Age and Growth of the Bull Shark in
782 the Western North Atlantic Ocean. Transactions of the American Fisheries Society 143, 732–
783 743. https://doi.org/10.1080/00028487.2014.892537
784 Perrot, V., Masbou, J., V. Pastukhov, M., N. Epov, V., Point, D., Bérail, S., R. Becker, P., E. Sonke, J.,
785 Amouroux, D., 2016. Natural Hg isotopic composition of different Hg compounds in mammal
786 tissues as a proxy for in vivo breakdown of toxic methylmercury. Metallomics 8, 170–178.
787 https://doi.org/10.1039/C5MT00286A
788 Perrot, V., Pastukhov, M.V., Epov, V.N., Husted, S., Donard, O.F.X., Amouroux, D., 2012. Higher Mass-
789 Independent Isotope Fractionation of Methylmercury in the Pelagic Food Web of Lake Baikal
790 (Russia). Environ. Sci. Technol. 46, 5902–5911. https://doi.org/10.1021/es204572g
791 Pethybridge, H., Choy, C.A., Logan, J.M., Allain, V., Lorrain, A., Bodin, N., Somes, C.J., Young, J.,
792 Ménard, F., Langlais, C., Duffy, L., Hobday, A.J., Kuhnert, P., Fry, B., Menkes, C., Olson, R.J.,
793 2018. A global meta-analysis of marine predator nitrogen stable isotopes: Relationships

between trophic structure and environmental conditions. Global Ecology and Biogeography 27, 1043–1055. https://doi.org/10.1111/geb.12763

Pethybridge, H., Cossa, D., Butler, E.C.V., 2010. Mercury in 16 demersal sharks from southeast Australia: Biotic and abiotic sources of variation and consumer health implications. Marine Environmental Research 69, 18–26. https://doi.org/10.1016/j.marenvres.2009.07.006

Roff, G., Brown, C.J., Priest, M.A., Mumby, P.J., 2018. Decline of coastal apex shark populations over the past half century. Communications Biology 1, 223. https://doi.org/10.1038/s42003-018-0233-1

Roff, G., Doropoulos, C., Rogers, A., Bozec, Y.-M., Krueck, N.C., Aurellado, E., Priest, M., Birrell, C., Mumby, P.J., 2016. The Ecological Role of Sharks on Coral Reefs. Trends in Ecology & Evolution 31, 395–407. https://doi.org/10.1016/j.tree.2016.02.014

Ruiz-de-Cenzano, M., Rochina-Marco, A., Cervera, M.L., de la Guardia, M., 2014. Speciation of methylmercury in market seafood by thermal degradation, amalgamation and atomic absorption spectroscopy. Ecotoxicology and Environmental Safety 107, 90–96. https://doi.org/10.1016/j.ecoenv.2014.05.015

Sackett, D.K., Drazen, J.C., Choy, C.A., Popp, B., Pitz, G.L., 2015. Mercury Sources and Trophic Ecology for Hawaiian Bottomfish. Environ. Sci. Technol. 49, 6909–6918. https://doi.org/10.1021/acs.est.5b01009

Sackett, D.K., Drazen, J.C., Popp, B.N., Choy, C.A., Blum, J.D., Johnson, M.W., 2017. Carbon, Nitrogen, and Mercury Isotope Evidence for the Biogeochemical History of Mercury in Hawaiian Marine Bottomfish. Environ. Sci. Technol. 51, 13976–13984. https://doi.org/10.1021/acs.est.7b04893

Sardenne, F., Hollanda, S., Lawrence, S., Albert-Arrisol, R., Degroote, M., Bodin, N., 2017. Trophic structures in tropical marine ecosystems: a comparative investigation using three different ecological tracers. Ecological Indicators 81, 315–324. https://doi.org/10.1016/j.ecolind.2017.06.001

Scheuhammer, A., Braune, B., Chan, H.M., Frouin, H., Krey, A., Letcher, R., Loseto, L., Noël, M., Ostertag, S., Ross, P., Wayland, M., 2015. Recent progress on our understanding of the biological effects of mercury in fish and wildlife in the Canadian Arctic. Science of The Total Environment, Special Issue: Mercury in Canada's North 509–510, 91–103. https://doi.org/10.1016/j.scitotenv.2014.05.142

Senn, D.B., Chesney, E.J., Blum, J.D., Bank, M.S., Maage, A., Shine, J.P., 2010. Stable isotope (N, C, Hg) study of methylmercury sources and trophic transfer in the northern gulf of Mexico. Environ. Sci. Technol. 44, 1630–1637. https://doi.org/10.1021/es902361j

Trystram, C., 2016. Écologie trophique de poissons prédateurs et contribution à l'étude des réseaux trophiques marins aux abords de La Réunion.

Trystram, C., Rogers, K.M., Soria, M.M., Jaquemet, S., 2016. Feeding patterns of two sympatric shark predators in coastal ecosystems of an oceanic island. Canadian Journal of Fisheries and Aquatic Sciences. https://doi.org/10.1139/cjfas-2016-0105

Trystram, C., Roos, D., Guyomard, D., Jaquemet, S., 2015. Mechanisms of trophic partitioning within two fish communities associated with a tropical oceanic island. Western Indian Ocean Journal of Marine Science 14, 93–111.

Tsui, M.T.-K., Blum, J.D., Kwon, S.Y., 2020. Review of stable mercury isotopes in ecology and biogeochemistry. Science of The Total Environment 716, 135386. https://doi.org/10.1016/j.scitotenv.2019.135386

Wang, X., Wu, F., Wang, W.-X., 2017. In Vivo Mercury Demethylation in a Marine Fish (Acanthopagrus schlegeli). Environ. Sci. Technol. 51, 6441–6451. https://doi.org/10.1021/acs.est.7b00923

Werry, J.M., Lee, S.Y., Lemckert, C.J., Otway, N.M., 2012. Natural or Artificial? Habitat-Use by the Bull Shark, Carcharhinus leucas. PLOS ONE 7, e49796. https://doi.org/10.1371/journal.pone.0049796

Werry, J.M., Lee, S.Y., Otway, N.M., Hu, Y., Sumpton, W., 2011. A multi-faceted approach for quantifying the estuarine–nearshore transition in the life cycle of the bull shark, Carcharhinus leucas. Mar. Freshwater Res. 62, 1421–1431. https://doi.org/10.1071/MF11136

Werry, J.M., Planes, S., Berumen, M.L., Lee, K.A., Braun, C.D., Clua, E., 2014. Reef-Fidelity and Migration of Tiger Sharks, Galeocerdo cuvier, across the Coral Sea. PLOS ONE 9, e83249. https://doi.org/10.1371/journal.pone.0083249

Zhang, Y., Jaeglé, L., Thompson, L., 2014. Natural biogeochemical cycle of mercury in a global three-dimensional ocean tracer model. Global Biogeochemical Cycles 28, 553–570. https://doi.org/10.1002/2014GB004814

Zheng, W., Foucher, D., Hintelmann, H., 2007. Mercury isotope fractionation during volatilization of Hg(0) from solution into the gas phase. Journal of Analytical Atomic Spectrometry 22, 1097–1104. https://doi.org/10.1039/B705677J

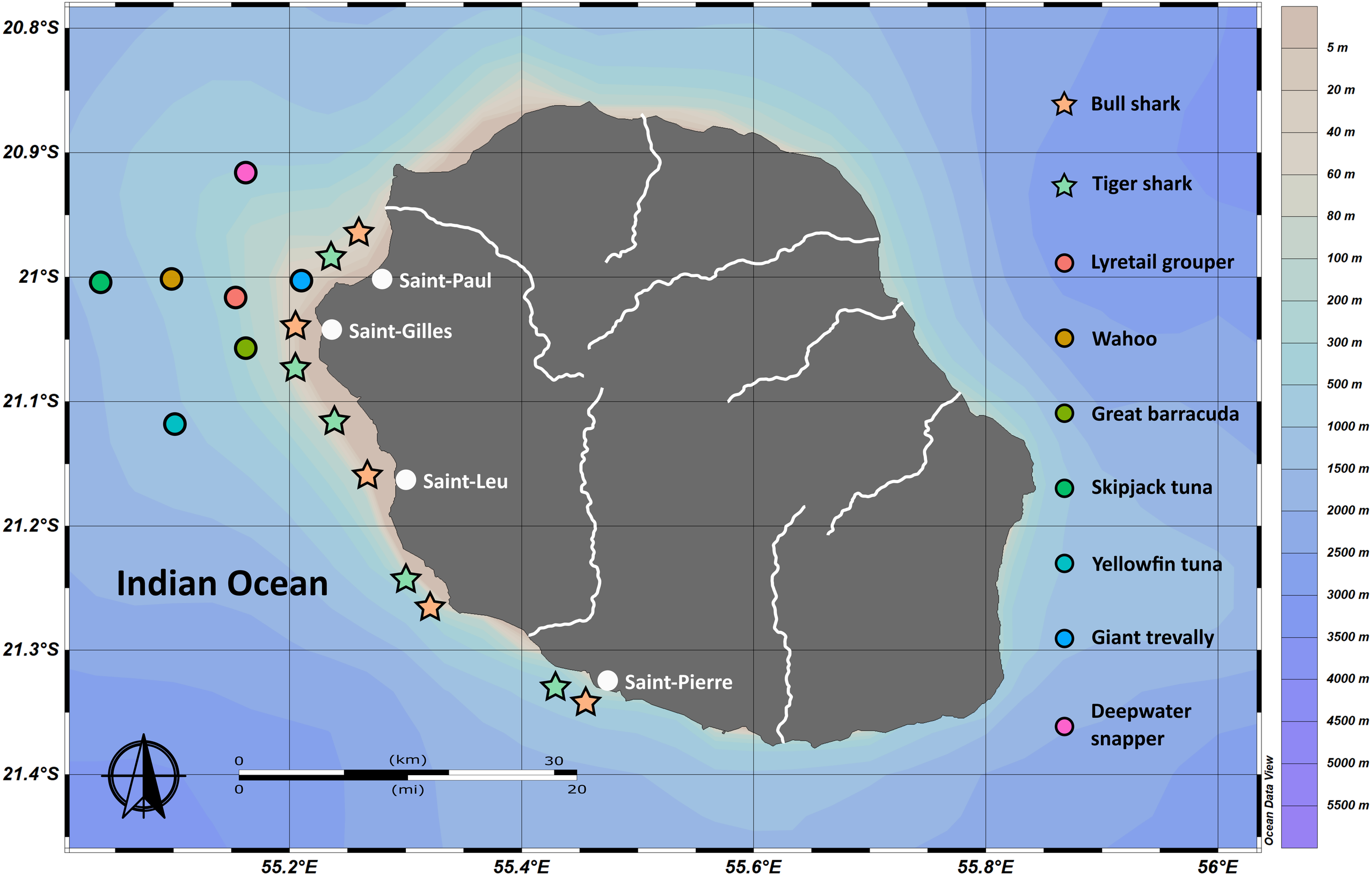
20.8°S
20.9°S
21°S
21.1°S
21.2°S
21.3°S
21.4°S
55.2°E
55.4°E
55.6°E
55.8°E
56°E
Saint-Paul
Saint-Gilles
Saint-Leu
Saint-Pierre
Indian Ocean
0
(km)
30
0
(mi)
20
Bull shark
Tiger shark
Lyretail grouper
Wahoo
Great barracuda
Skipjack tuna
Yellowfin tuna
Giant trevally
Deepwater snapper
5 m
20 m
40 m
60 m
80 m
100 m
200 m
300 m
500 m
1000 m
1500 m
2000 m
2500 m
3000 m
3500 m
4000 m
4500 m
5000 m
5500 m
Ocean Data View

A

muscle Δ^{199}Hg (‰)

3.0
2.5
2.0
1.5

Bull

Tiger

B

muscle δ^{202}Hg (‰)

2.5
2.0
1.5
1.0
0.5
0.0

Bull

Tiger

+1.4‰

Demethylation

+1.1‰

Lyretail grouper
Wahoo
Great barracuda
Skipjack tuna
Yellowfin tuna
Giant trevally
Lantern fish
Deepwater snapper

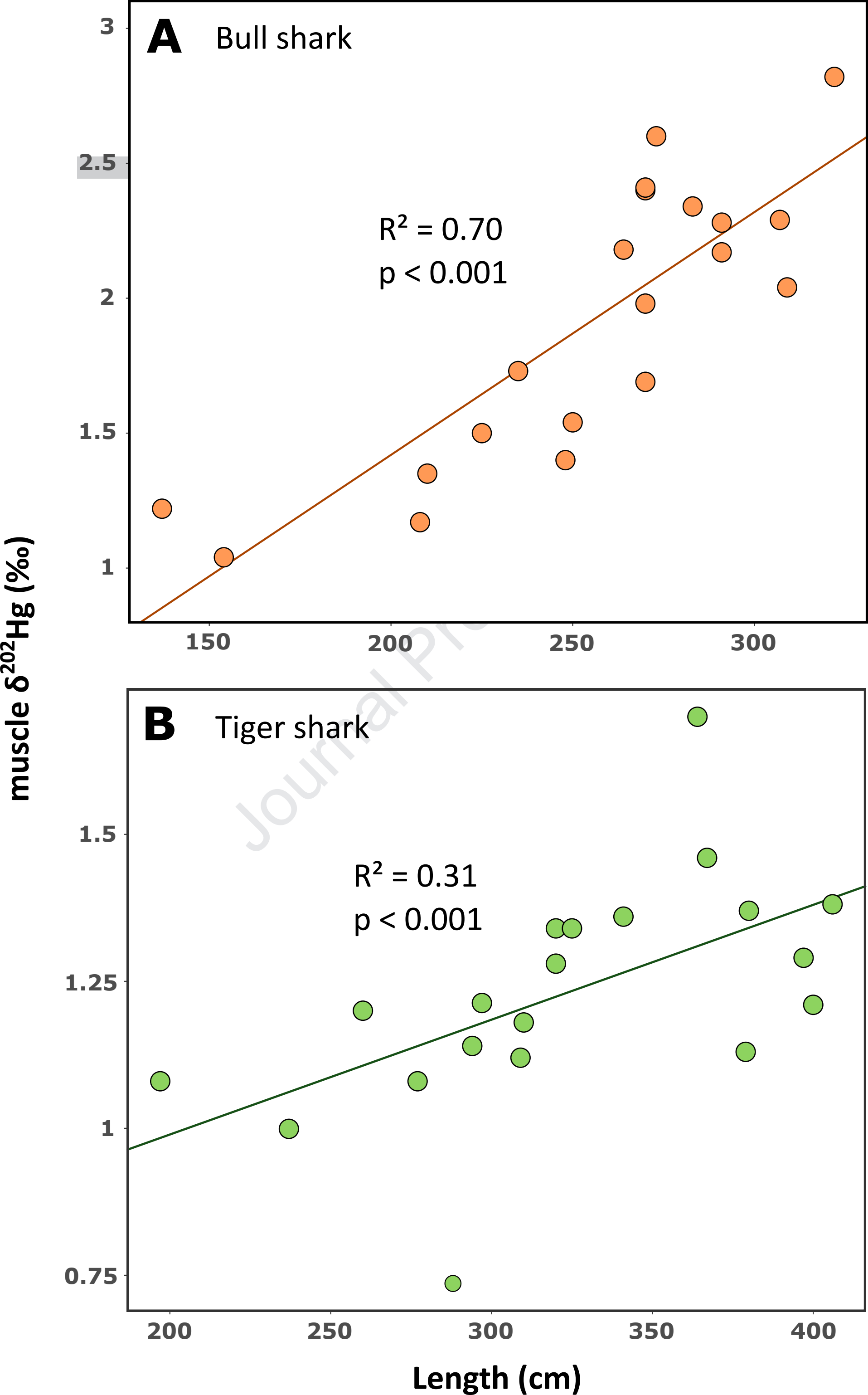
A
Bull shark
R² = 0.70
p < 0.001
3
2.5
2
1.5
1
150
200
250
300
B
Tiger shark
R² = 0.31
p < 0.001
1.5
1.25
1
0.75
200
250
300
350
400
Length (cm)
muscle δ202Hg (‰)

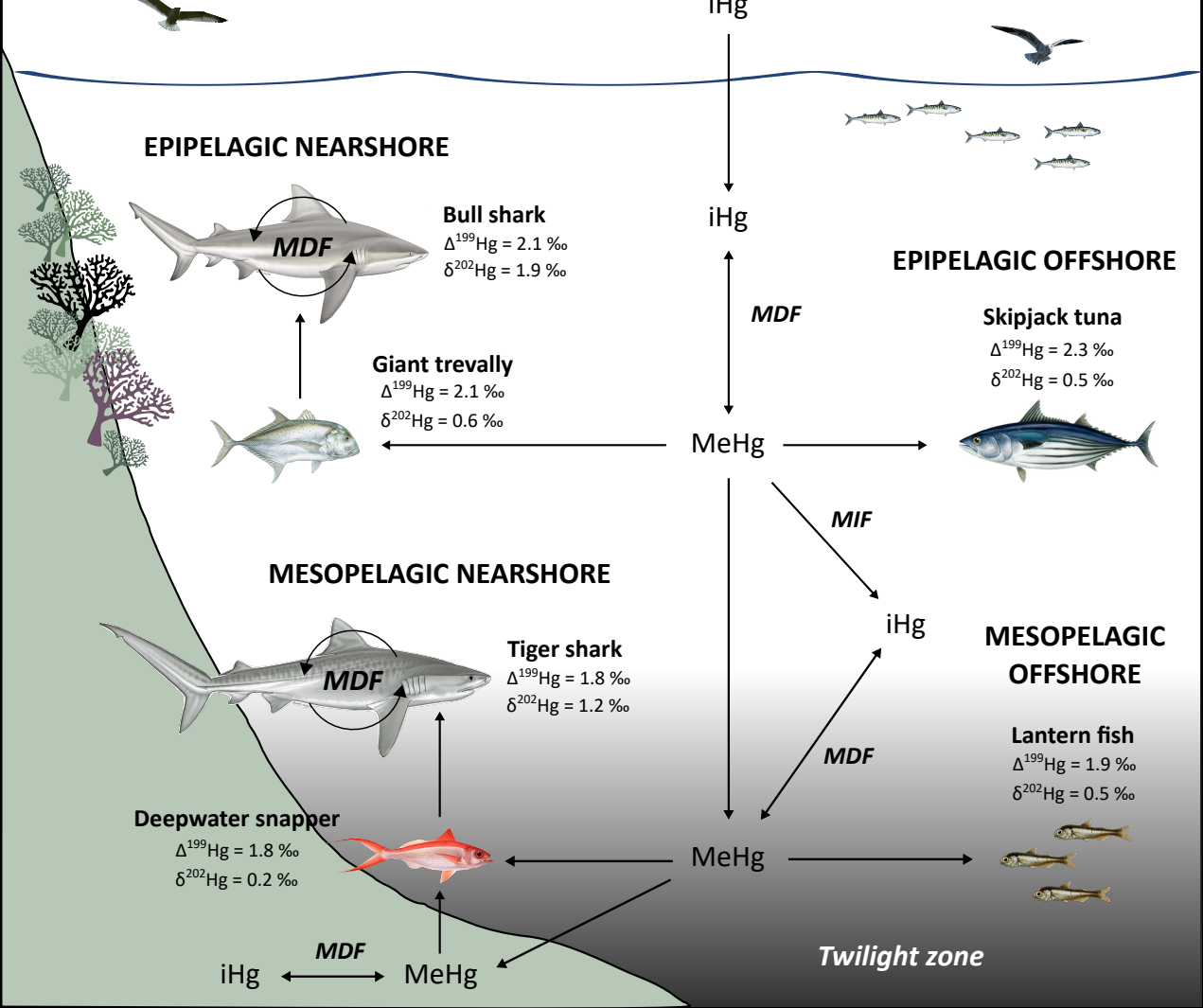
iHg
EPIPELAGIC NEARSHORE
MDF
Bull shark
Δ199Hg = 2.1 ‰
δ202Hg = 1.9 ‰
iHg
EPIPELAGIC OFFSHORE
MDF
Skipjack tuna
Δ199Hg = 2.3 ‰
δ202Hg = 0.5 ‰
Giant trevally
Δ199Hg = 2.1 ‰
δ202Hg = 0.6 ‰
MeHg
MIF
MESOPELAGIC NEARSHORE
iHg
MESOPELAGIC OFFSHORE
MDF
Tiger shark
Δ199Hg = 1.8 ‰
δ202Hg = 1.2 ‰
MDF
Lantern fish
Δ199Hg = 1.9 ‰
δ202Hg = 0.5 ‰
Deepwater snapper
Δ199Hg = 1.8 ‰
δ202Hg = 0.2 ‰
MeHg
MDF
iHg
MeHg
Twilight zone

Figure captions

Figure 1: Map of sampling locations of the shark and prey species along the west coast of La Réunion Island. Major rivers are figured in white lines. Lantern fish are not shown but were caught in the area (off La Réunion Island and off southern Madagascar).

Figure 2: A: Δ^{199}Hg (‰) in the bull shark (orange bar, mean ± SD), the tiger shark (green bar, mean ± SD) and prey species (dots, mean ± SD) from La Réunion Island. The prey fish are ordered according to their Δ^{199}Hg values. The bull shark had higher (ANOVA, $p < 0.001$) Δ^{199}Hg than the tiger shark. The bull shark shared similar Δ^{199}Hg with the yellowfin tuna and the giant trevally while the tiger shark shared similar Δ^{199}Hg with the deepwater snapper.
B: δ^{202}Hg (‰) in the bull shark (orange bar, mean ± SD), the tiger shark (green bar, mean ± SD) and prey species (dots, mean ± SD). Bull shark had higher (KW, $p < 0.001$) and more variable (Bartlett test, $p < 0.001$) δ^{202}Hg than tiger shark. Bull shark had higher δ^{202}Hg than its prey (e.g. giant trevally; KW, $p < 0.001$). Similarly, the tiger shark displayed higher δ^{202}Hg than its prey (e.g. deepwater snapper; ANOVA, $p < 0.001$).

Figure 3: Muscle δ^{202}Hg values versus total length for the bull shark (**A**) and the tiger shark (**B**). Data fits a linear regression in A and B.

Figure 4: Simplified representation of the Hg cycle in the environment of bull and tiger sharks. Atmospheric inorganic Hg (iHg) is deposited to water before being methylated to methyl-Hg (MeHg) along the water column, which induces mass-dependent fractionation (MDF). MeHg can then be demethylated by solar radiation in the photic zone of the water column, inducing mass-independent fractionation (MIF). Hg can reach the deep layers trough particle sinking, either in the MeHg form, or in the iHg form. iHg can also be methylated in the twilight zone. Epipelagic MeHg is directly incorporated into the bull shark food web, while the tiger shark food web is exposed to a mixed pool of (i) mesopelagic offshore MeHg and (ii) benthic MeHg subject to bacterial transformation in slope sediments. MeHg is finally demethylated in sharks, leading to high δ^{202}Hg values. Reduction of iHg into gaseous Hg^0 and subsequent volatilization is not represented.

Highlights:

Mercury isotopes were analyzed in bull and tiger sharks from the Indian Ocean

Hg MIF signature revealed that bull sharks target coastal prey in shallow water

Δ^{199}Hg values showed that tiger sharks forage on deeper habitat on the island slope

δ^{202}Hg shift between prey and predator may indicate MeHg demethylation in sharks

Declaration of interests

☒ The authors declare that they have no known competing financial interests or personal relationships that could have appeared to influence the work reported in this paper.

☐The authors declare the following financial interests/personal relationships which may be considered as potential competing interests: